

## THE DEVELOPMENT OF PERFORMANCE PREDICTION METHODS FOR AN AUTOMOTIVE CO<sub>2</sub> AIR CONDITIONING CYCLE

**Masafumi Katsuta**  
Waseda University  
Shinjuku, Tokyo, JAPAN

**Takahiro Oshiro**  
Graduate School of Waseda Uni  
Shinjuku, Tokyo, JAPAN

**Akira Kaneko**  
Graduate School of Waseda Uni  
Honjoh, Saitama, JAPAN

**Sangchul BAE**  
Waseda University  
Honjoh, Saitama, JAPAN

**Shunji Komatsu**  
Waseda University  
Shinjuku, Tokyo, JAPAN

**Yohei Ohno**  
Graduate School of Waseda Uni  
Shinjuku, Tokyo, JAPAN

### ABSTRACT

In previous researches, we have been focusing on the performance of the each element heat transfer and hydraulic performance of refrigeration cycle. Experimental investigations have been repeated several times and, finally, we have substantial data base including the effect of lubricant oil. Moreover, the mal-distribution of two-phase in an evaporator can be also predicted from the experimental data base. Under these circumstances, this study is intended to effectively put the construction of an automotive CO<sub>2</sub> air conditioning system into practical design use through the simulation using the above-mentioned data base.

This paper describes the refrigeration cycle performance prediction of each element (e.g. an evaporator, a gas-cooler, and so on) by a simulation using substantial data base and various available correlations proposed by us and several other researchers. In the performance prediction model of heat exchangers, local heat transfer and flow characteristics are considered and in addition, the effects of lubricant oil on heat transfer and pressure drop are duly considered.

The comparison is also made between simulation results and bench test results using a real automotive air conditioning system. Finally, the developed simulation method can predict the cooling ability successfully within  $\pm 5\%$ . By incorporating the lubricant oil effect, the simulation results are improved to  $\pm 5\%$  and  $\pm 15\%$  for the cooling ability and pressure drop respectively.

### INTRODUCTION

Due to the increasing environmental concern, the reduction of greenhouse effect gas, particularly, CO<sub>2</sub> emission and the direct leak of HCFC and HFC's have been considered to be among most important subjects in the field of refrigeration and air-conditioning system. At present, the demand for the higher efficiency of a refrigeration system (COP) increases. More

recently, the possibility of global warming potential (GWP) is extremely large, and the conventional refrigerant can go ahead through the policy that does not recognize a chlorofluorocarbon alternative to the refrigerant for car air-conditioners positively in EU particular, and the interest for natural refrigerant increases.

Among various candidates of natural refrigerants, CO<sub>2</sub> is environmentally safe, being not toxic and non-flammable, so CO<sub>2</sub> has advantages for practical reasons. Moreover, CO<sub>2</sub> possesses a low viscosity, high specific heat, and high thermal conductivity. In general, it has excellent thermodynamic and transport properties as a refrigerant.

On the other hand, however, since CO<sub>2</sub> has high critical pressure and its critical temperature is low, it becomes a trans-critical cycle and the COP becomes low when compared with conventional refrigerants. Therefore, the high efficiency of heat exchangers is inevitable and it is necessary to grasp the plenary heat transfer coefficients and the basic characteristics of pressure drop in an evaporator and in a gas cooler. Moreover, it presents other problems; for example, the performance deteriorates because the lubricant oil contaminates into the refrigerant in a real working system. So various efforts have been made to investigate these aspects.

Although a lot of evaporation heat transfer data are available in literature (Koyama 2004<sup>(1)</sup>, Yamada 2004<sup>(2)</sup>, Katsuta 2006<sup>(3)</sup>) and it is recognized that the evaporation heat transfer is very sensitive for lubricant oil concentration rate (OCR), few investigations have addressed to the effect of OCR and its prediction. The objective of this research, therefore, is to investigate the effect of oil mixing rate on the thermal and hydraulic characteristics using CO<sub>2</sub> as working refrigerant.

In previous researches, we have been focusing on the performance of the each element heat transfer and hydraulic performance. Experimental investigations have been repeated several times and, finally, we have substantial data base

including the effect of lubricant oil. Moreover, the mal-distribution of two-phase in an evaporator can be also predicted from the experimental data base.

This paper describes the refrigeration cycle performance prediction of each element by a simulation using substantial data base and various available correlations proposed by us and several other researchers. In the performance prediction model of heat exchangers, local heat transfer and flow characteristics are considered and in addition, the effects of lubricant oil on heat transfer and pressure drop are duly considered.

Also, the comparison is made between simulation results and bench test results using a real automotive air conditioning system.

## THE EXPERIMENTAL CORRELATIONS EMPLOYED IN THIS SIMULATION

### PRESSURE DROP

In this simulation, we adopt the previously proposed pressure drop correlation in term of the Lockhart and Martinelli parameter expression. It is well-known that the pressure drop of the two-phase flow in a horizontal tube is composed of two terms, namely the friction loss and the acceleration loss. The former term describes as Eq. (2). The two phase multiplier used in the prediction of the latter term is evaluated from Eq. (3). In addition, to propose the empirical correlation covered throughout quality (from 0 to 1), other terms to correct the two phase flow pattern and the maximum pressure drop are added.

$$\left(\frac{\Delta P}{\Delta L}\right) = \left(\frac{\Delta P}{\Delta L}\right)_f + \left(\frac{\Delta P}{\Delta L}\right)_{ac} \quad (1)$$

$$\left(\frac{\Delta P}{\Delta L}\right)_{ac} = G^2 \left\{ \left[ \frac{x_{out}^2}{\alpha_{out} \rho_g} + \frac{(1-x_{out})^2}{(1-\alpha_{out}) \rho_l} \right] - \left[ \frac{x_{in}^2}{\alpha_{in} \rho_g} + \frac{(1-x_{in})^2}{(1-\alpha_{in}) \rho_l} \right] \right\} \quad (2)$$

$$\psi = 1 + \left( S \frac{1-x}{x} \frac{\rho_g}{\rho_l} \right)$$

$$S = 1 + E_1 \left( \frac{y}{1+yE_2} - yE_2 \right)^{0.5}$$

$$y = \frac{\beta}{1-\beta}$$

$$E_1 = 1.578 \text{Re}_{l,0}^{-0.19} \left( \frac{\rho_g}{\rho_l} \right)^{0.22}$$

$$E_2 = 0.0273 \text{We}_{l,0}^{-0.51} \left( \frac{\rho_g}{\rho_l} \right)^{-0.08}$$

$$\beta = \frac{\rho_l x}{\rho_l x + \rho_g (1-x)}$$

$$\text{Re}_{l,0} = \frac{GD}{\mu_l}$$

$$\text{We} = \frac{G^2 D}{\sigma \rho_l}$$

$$\left(\frac{\Delta P}{\Delta L}\right)_f = \left(\frac{\Delta P}{\Delta L}\right)_{10} \times \beta_1 \times \phi_{10}^2$$

$$\left(\frac{\Delta P}{\Delta L}\right)_{10} = \frac{2fG^2}{D\rho_l}$$

$$f = 0.079 / \text{Re}_l^{0.25}$$

Slug or Froth

$$\phi_{10}^2 = \left( -0.1667 \times \ln \left( \frac{1}{X_n} \right) + 21.13 \right) \times \left( \frac{\rho_l}{\rho_g} \right)^{5.34} \left( \frac{\mu_g}{\mu_l} \right)^{7.32} \text{Re}_l^{-0.2904} Fr_x^{0.422} \eta_1 \times \omega$$

$$Bd < 30 \quad \eta_1 = 27.89 Bd^{-0.01141}$$

$$Bd \geq 30 \quad \eta_1 = 1.623 Bd^{0.607}$$

Annular

$$\phi_{10}^2 = \left( 3.26 \times \ln \left( \frac{1}{X_n} \right) + 4.375 \right) \times \left( \frac{\rho_l}{\rho_g} \right)^{5.102} \left( \frac{\mu_g}{\mu_l} \right)^{6.848} \text{Re}_l^{0.2345} \eta_2 \times \omega \quad (3)$$

$$Bd < 30 \quad \eta_2 = 3.66 Bd^{-0.4518}$$

$$Bd \geq 30 \quad \eta_2 = 0.7344 Bd^{-0.1025}$$

$$x_d = \left( 0.393 \times \exp(-36.62 \times OCR) \times \text{Re}_l^{0.09133} Bd^{-0.01037} \right)$$

$$\beta_1 = 1$$

$$x_{local} > x_d$$

$$\beta_1 = 1 + 394.9 \left( 1617 - 366.4 \times \ln \left( \frac{1}{X_n} \right) \times Bd^{0.6011} \text{Re}_l^{-1.226} OCR^{1.249} \right)$$

$$x_{local} < x_d$$

$$\text{Re}_l = \frac{GD(1-x)}{\mu_l}$$

$$Fr_x = \frac{Gx}{\sqrt{\rho_g (\rho_l - \rho_g) Dg}}$$

$$Bd = \frac{g(\rho_l - \rho_g) D^2}{\sigma}$$

### HEAT TRANSFER

Because in recent open references to the evaporation heat transfer, various correlations based on Chen's type (Chen, 1996) were proposed and successfully predicted the trend of experimental data, it is very important which kind of correlations are applied in this simulation. In this simulation we decide to adopt our proposed heat transfer correlation, which is taking into account the effect of oil contamination. These correlations are based on our accumulated data base in long term experimental research. Our empirical evaporating heat transfer correlations are explained as follows: Chen's type, Katsuta et al., 2006.

Our proposed heat transfer correlation was also based on the following Chen's type, the evaporating convective heat transfer can represents the superposition of convective and boiling heat transfer.

$$\alpha = \alpha_{con} + \alpha_{bo} \quad (4)$$

In Eq.(5) and (6), convective heat transfer term and nucleate boiling heat transfer term are given as follows;

$$\alpha_{con} = F \times 0.023 \frac{\lambda_l}{D} \left( \frac{G(1-x)D}{\mu_l} \right)^{0.8} \text{Pr}^{0.4} \quad (5)$$

$$F = 1 + 0.258 \times \left( \frac{1}{X_n} \right)^{0.886} + 92.32 \left( \frac{\rho_g}{\rho_l} \right)^3 \left( \frac{1}{X_n} \right)^{0.9} \quad (\text{Without Oil})$$

$$\alpha_{bo} = S' \alpha_{SA}$$

$$\alpha_{SA} = 207 \frac{\lambda_l}{D_b} \left( \frac{qD_b}{\lambda_l T_{sat}} \right)^{0.745} \left( \frac{\rho_g}{\rho_l} \right)^{0.581} \text{Pr}_f^{0.533} \quad (6)$$

$$S' = 5 \exp \left\{ -5 \times 10^{-5} \times \left( 0.1 \times \frac{\text{Re}_{sp} \times 10^8}{Bo^{0.1}} \right)^{0.4} \right\} \quad (\text{Without Oil})$$

$$\gamma = 1 + 3 \exp \left\{ -0.006 \times Bo \times 10^4 \times (Bd \times Fr)^{1.3} \right\}$$

Based on the qualitative trend of evaporation heat transfer, to take into account the local oil concentration and the evaporation temperature, the convection enhanced factor  $F$  is modified as Eqs.(5) and (7). On the other hand, the nucleate boiling suppression factor  $S$  in considering the effect of heat flux and the latent heat of evaporation, namely Boiling number, is revealed as Eqs.(6) and (8).

$$\alpha_{con} = F \times 0.023 \frac{\lambda_l}{D} \left( \frac{G(1-x)D}{\mu_l} \right)^{0.8} Pr^{0.4} \quad (7)$$

$$F = 1 + 6.40 \times \left( \frac{1}{X_{tt}} \right)^{0.770} \left( \frac{\rho_v}{\rho_l} \right)^{0.581} \quad (\text{With Oil})$$

$$\alpha_{bo} = S' \alpha_{SA}$$

$$\alpha_{SA} = 207 \frac{\lambda_l}{D_b} \left( \frac{q D_b}{\lambda_l T_{sat}} \right)^{0.745} \left( \frac{\rho_v}{\rho_l} \right)^{0.581} Pr_l^{0.533} \quad (8)$$

$$S' = \ln \left( 2332 \frac{Bo^{0.518} Bd^{1.27} Fr^{0.964}}{Re_{fp}^{0.834}} \right) \quad (\text{With Oil})$$

To establish the heat transfer prediction including the oil contamination effect, the heat transfer due to this effect is introduced here. By using the heat flux, latent heat of evaporation and surface tension, these are the major contribution factors to deteriorate the nucleate boiling heat transfer, the following dimensionless groups (Boiling Number and Bond Number) are taken into account;

$$\alpha_{bo} = S' \alpha_{SA} \times \phi'$$

$$\phi' = \frac{1}{(1 + OCR^{0.698} Bo^{0.207} Bd^{0.912})} \quad (9)$$

## THE EVAPORATOR SIMULATION MODEL

The objective of applied this simulation is evaporator referred as S-type and B-type supplied by two companies and S-type evaporator is shown in Fig.3

An evaporator simulation and calculation procedure is as follows; an evaporator is divided into 20 segments which has equal in length ( $dL$ ) along the refrigerant flow direction and each segments deal with an independent minute heat exchanger. The calculation is performed from outlet to inlet condition under assuming the constant heat transfer coefficient and taking into account the energy balance in the segment.

First, the specification of the evaporator and the quantity of the heat exchanger outlet refrigerant state and the inlet of outside air state from experimental data (from prototype bench test) are provided. Then, judging from segment assumed inlet refrigerant pressure and enthalpy, a decision of refrigeration vapor being saturated or superheated is made. Assuming the inlet quality or the temperature of the segment, the pressure drop of the refrigerant side is calculated and we estimate the heat transfer rate of the segment from the refrigerant side energy balance as referred as  $dQ_{fake1}$  is estimated.

After the above-mentioned procedure, calculated heat transfer rate from refrigerant heat transfer coefficient  $dQ_{fake2}$  is followed. A judgment whether the outside heat transfer tube wet or dry is made from the estimated air side outlet temperature. The outside heat transfer tube wall temperature can be evaluated using  $dQ_{fake1}$  and then  $dQ_{fake2}$  is estimated.

As shown in the simulation flow chart (Fig.1), this calculation procedure is repeated with correcting segment inlet refrigeration quality of state until it satisfy the following convergence condition  $dQ_{fake1} = dQ_{fake2}$ .

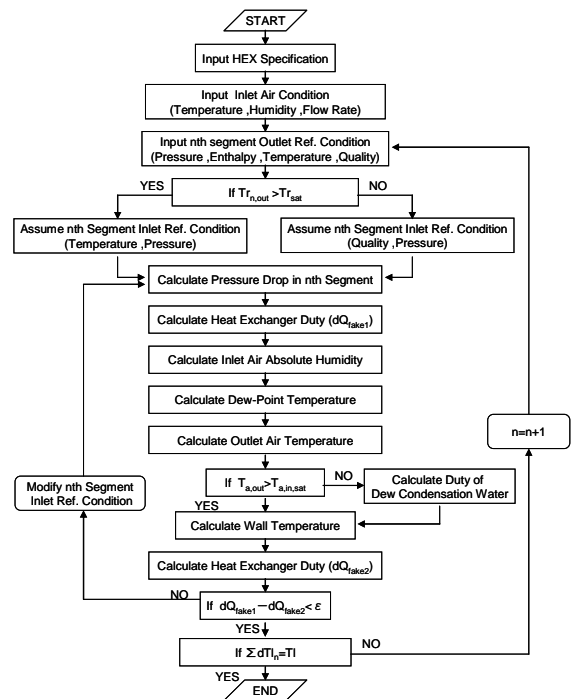


Fig.1 Flowchart of Evaporator Simulation

## CYCLE SIMULATION WITHOUT INTERNAL HEAT EXCHANGER

A cycle simulation and calculation procedure without internal heat exchanger is as follows: First the specification of evaporator, the gas cooler and the compressor are provided, after that, the calculation condition is fixed by entering the air side heat source condition (e.g. temperature, humidity and air flow rate) and compressor suction side superheat. Then, assuming the evaporator outlet pressure and pressure ratio, the inlet and outlet states of the compressor are calculated. The outlet state of the gas cooler are calculated using gas cooler HX simulation program and the pressure ratio is modified as if these state are achieved the optimum COP. Theoretically, this calculation procedure is repeated until its satisfy the pressure ratio convergence condition. When the convergence is completed, the inlet state of evaporator is evaluated using the above-mentioned evaporator simulation method and the judgment of agreement between this state and the outlet state of the expansion valve is made. If the data disagrees, the calculation procedure is repeated correcting the outlet pressure of the evaporator.

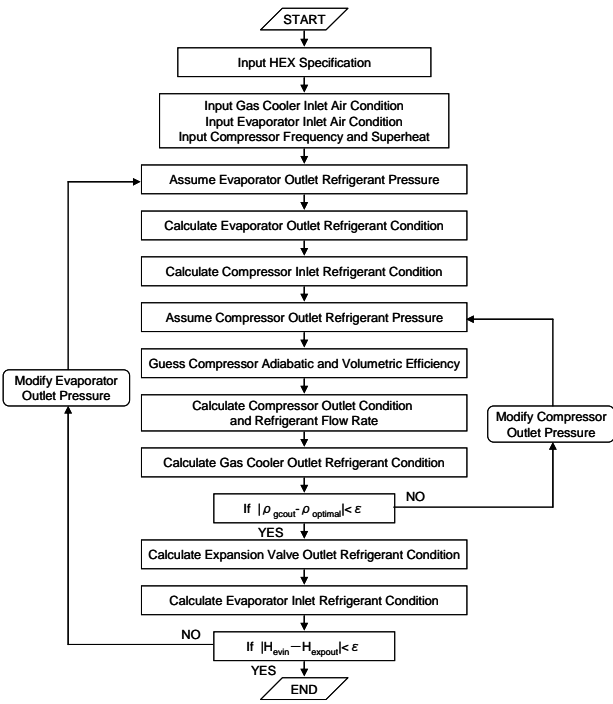


Fig.2 Flowchart of Cycle Simulation

**SIMULATION RESULTS AND DISCUSSION**  
**SPECIFICATIONS OF A PRACTICAL EVAPORATOR**  
**APPLYING THIS SIMULATION METHOD AND BENCH**  
**TEST EXPERIMENTAL CONDITIONS**

The objective of applying this simulation is evaporators supplied by two companies (referred as S-type and B-type) and an exterior structure of S-type evaporator is shown in Fig. 3. Additionally, Table1 shows the detailed specifications of S-type and Table 3 shows B-type evaporators. Please note that the inner geometry of B-type is an unknown factor, so the inside specification are supposed from the measured outside temperature distribution by a radiation thermometer. Table 2 and Table 4 show experimental conditions of S-type and B-type, respectively.

Table1 Evaporator Specification (S-type)

Name	Specification	Unit
Overall Size	245 × 263 × 38	mm
Core Size	211.5 × 263	mm
Number of Tubes (Pass1/Pass2/Pass3) (Pass4/Pass5/Pass6)	12 / 12 / 12 12 / 12 / 12	
Tube Width	15	mm
Tube Thickness	1.1	mm
Number of Ports	18	
Hydraulic Diameter	0.5	mm
Fin Height	6	mm
Fin Pitch	1.5	mm
Fin Width	38	mm
Fin Thickness	0.08	mm

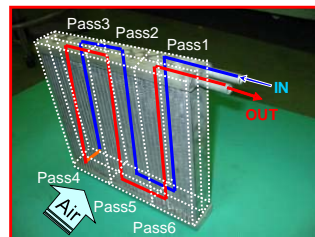


Fig.3 Structure of Evaporator

Table2 Experimental Conditions (S-type)

TestNo.	A2	A3	A4	B1	B2	B3	B4	C1	C2	C3	C4
Air Temp. (DB) °C	27										
Air Temp. (WB) °C	19.53										
Outlet Refrigerant Press. MPaG	3.29										
Outlet Superheat °C	not over 3 deg										
Expansion Valve Inlet Press. MPaG	9			10			11				
Expansion Valve Inlet Temp. °C	30			35			40				
Air Flow Rate m³/h	300	400	500	200	300	400	500	200	300	400	500
Predicted OCR wt. %	3.71	5.27	19.4	2.4	13.3	22.7	23.6	19.5	24.7	25.6	25.1

TestNo.	D1	D2	D3	D4	E2	E3	E4
Air Temp. (DB) °C	27						
Air Temp. (WB) °C	19.53						
Outlet Refrigerant Press. MPaG	3.29						
Outlet Superheat °C	not over 3 deg						
Expansion Valve Inlet Press. MPaG	9						
Expansion Valve Inlet Temp. °C	35			40			
Air Flow Rate m³/h	200	300	400	500	300	400	500
Predicted OCR wt. %	0.41	5.80	11.7	18.5	5.51	16.6	21.3

Table3 Evaporator specifications (B-type)

Name	Specification	Unit	Name	Specification	Unit
Overall Size	235 × 265 × 40	mm	Number of Tubes (Pass1/Pass2/Pass3) (Pass4/Pass5/Pass6)	8 / 9 / 9 9 / 9 / 8	
Core Size	215 × 260	Mm		Port Diameter	0.8
Number of Tubes	26		Number of Ports		12
Fin Height	8	mm			
Fin Pitch	1.7	mm			
Tube Thickness	1.7	mm			

Table4 Experimental Conditions (B-type)

Test Condition	(A)	(B)	(C)	(D)	(E)	(F)	(G)	(H)	(I)	(J)	(K)	(L)
Evaporator Inlet Air DB °C	27											
Evaporator Inlet Air WB °C	19.53											
Evaporator Outlet Refrigerant Pressure MPaG	3.29											
Evaporator Outlet Superheat °C	not over 3 deg.											
Expansion Valve Inlet Pressure MPaG	9			10			11					
Expansion Valve Inlet Temperature °C	30			35			40					
Evaporator Inlet Air Flow Rate m³/h	200	300	400	500	200	300	400	500	200	300	400	500
Predicted OCR wt%	15.3	6.2	5.2	8.2	14.1	9.7	9.6	12.4	11.3	2.4	6.9	7.3

**AIR SIDE HEAT TRANSFER CORRELATION**

Fig.4 shows air side HX configuration having Multi-Louvered fin type. To predict the outside heat transfer, we used the following Chang and Wang's correlation<sup>(5)</sup> 1997. They proposed following power series correlation for Colburn J factor with respect to fin geometry as a parameter. These correlations are available both dry and wet conditions. Fin efficiencies are also predicted as following expressions.

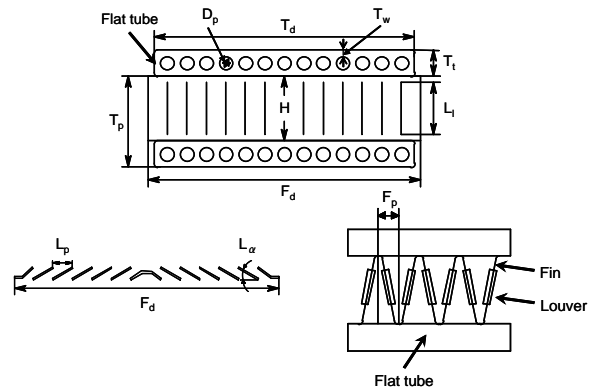


Fig.4 Schematic of Evaporator

### Dry Condition

$$j_{dry} = \text{Re}_{Lp}^{-0.487} \left(\frac{L_a}{90}\right)^{0.257} \left(\frac{F_p}{L_p}\right)^{-0.13} \left(\frac{H}{L_p}\right)^{-0.29} \left(\frac{F_d}{L_p}\right)^{-0.235} \left(\frac{L_l}{L_p}\right)^{0.68} \left(\frac{T_p}{L_p}\right)^{-0.279} \left(\frac{\delta_f}{L_p}\right)^{-0.05}$$

(100 ≤ Re<sub>Lp</sub> ≤ 600    F<sub>p</sub> / L<sub>p</sub> < 1)

### Wet Condition

$$j_{wet} = \text{Re}_{Lp}^{-0.512} \left(\frac{L_a}{90}\right)^{0.25} \left(\frac{F_p}{L_p}\right)^{-0.171} \left(\frac{H}{L_p}\right)^{-0.29} \left(\frac{F_d}{L_p}\right)^{-0.248} \left(\frac{L_l}{L_p}\right)^{0.68} \left(\frac{T_p}{L_p}\right)^{-0.275} \left(\frac{\delta_f}{L_p}\right)^{-0.05}$$

$$j = \frac{\alpha_o}{\rho_{air} V_{air} C_{p,air}} \text{Pr}^{\frac{2}{3}} \quad (80 \leq \text{Re}_{Lp} \leq 300 \quad F_p / L_p < 1)$$

## EFFECT OF THE TWO-PHASE FLOW DISTRIBUTION AT THE HEADER ON THE PERFORMANCE

First, to ensure the effect of the two-phase mal-distribution at the header, the comparison between a case with this effect considered and that this effect unconsidered is made by using Koyama<sup>(6)</sup> published report on R134a mal-distribution experimental results. To take into account this result applying different refrigerant, for example CO<sub>2</sub>, we decide that the key factor to dominate this phenomenon is a two-phase flow pattern in the header before separation. Using modified Baker two-phase flow pattern map, the CO<sub>2</sub> equivalent flow condition is identified from R134a data. The simulation and comparison results concerning S-type evaporator cooling capacity and pressure drop are represented from Fig.6. It is recognized that this effect is restricted, because simulation results of two cases almost coincide and especially as for the pressure drop, the simulation cannot predict measured data sufficiently and underestimates the measured data as 25%. From this, we should look for another factor to correct the disagreement.

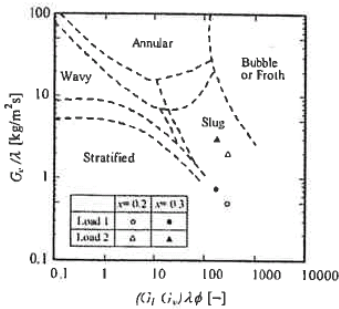


Fig.5 Modified Baker Flow Pattern Map with Koyama's Exp.

	CO2	HFC134a
P(MPa)	3.5	0.6
w(kg/h)	20	28.8
x	0.3	0.13

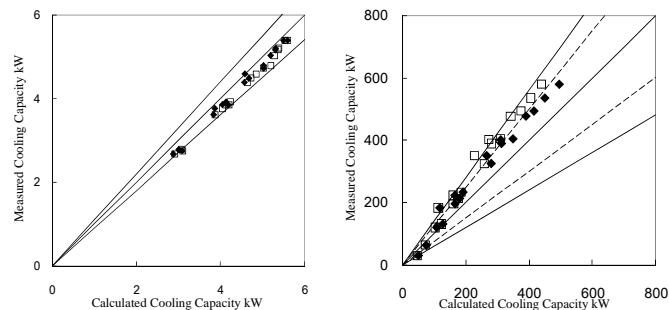


Fig.6 Prediction accuracy of Measured and Calculated Values

□: No consideration of flow distribution    ◆: Consideration of flow distribution

## THE EFFECT OF LUBRICANT OIL CONCENTRATION ON THE PERFORMANCE

Next, the simulation taking the OCR effect into consideration is made and the results are shown in Figs.7 and 8. In Addition OCR is measured value which is considered 0~4wt%. As shown in these figures, the simulation results for a S-type evaporator fairly improve both heat transfer and hydraulic characteristics. The accuracy of simulation is improved from ±10% to ±5% for cooling capacity and from ±40% to ±15% for pressure drop. The same simulation including OCR effect is also applied to the B-type evaporator. Regardless of different geometry, the simulation results predict the measured data successfully with almost the same accuracy as that of the C-type evaporator. In other words, it is recognized that the OCR plays an important part to estimate the evaporator performance and the availability of this simulation method is validated.

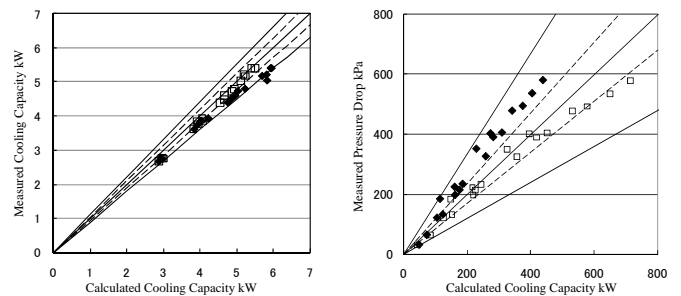


Fig.7 Prediction accuracy of Measured and Calculated Values

◆: No consideration of lubricant oil    □: Consideration of lubricant oil

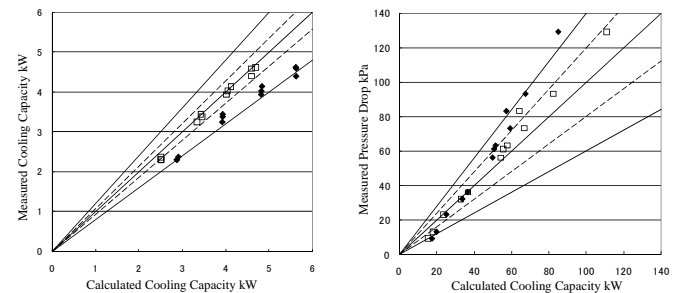


Fig.8 Prediction accuracy of Measured and Calculated Values

◆: No consideration of lubricant oil    □: Consideration of lubricant oil

## RESULTS OF CYCLE SIMULATION

The cycle simulation integrated each component (the flow chart is shown in Fig.2) is made and the results are shown in Fig.8. The cooling capacity, COP, the pressure drop and the compressor power are obtained and the comparison is made with the real cycle bench test, and moreover, the comparison between the pure CO<sub>2</sub> cycle (indicated as solid symbol) and including both of lubricant oil and two-phase flow distribution effect (indicated hollow symbol) are also made. From this figure, it is recognized that the cycle simulation accuracy

taking the OCR and flow distribution into consideration are much better than the pure CO<sub>2</sub> cycle.

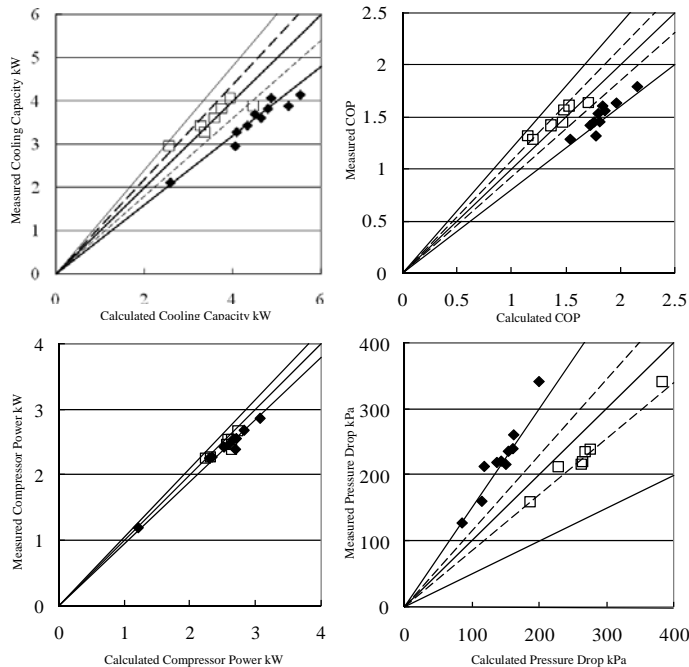


Fig.9 Comparison of Measured and Calculated Results (Cycle Simulation)

◆: No consideration of lubricant oil □: Consideration of lubricant oil

## CONCLUSIONS

### 1. The two-phase distribution at the header

Through taking the flow distribution of two-phase refrigerant at the header of each branches into account, the cooling capacity of the evaporator is increased on accuracy from  $\pm 10\%$  to  $\pm 5\%$  and, in several conditions of pressure loss, from  $\pm 40\%$  to  $\pm 25\%$ .

However, the improved accuracy is not enough even after the integration of predicted results of CO<sub>2</sub> distribution at the header.

### 2. The effect of lubricant oil on the evaporator simulation

By taking the effect of lubricant oil on the evaporator performance into account, the cooling capacity of the evaporator improved from  $\pm 10\%$  to  $\pm 5\%$ , the pressure loss improved from  $\pm 40\%$  to  $\pm 15\%$  in its accuracy.

### 3. The simulation applied to the different type evaporator

The evaporator simulation with lubricant oil is applied to the different type model and is predicted its performance successfully. From this, the validity of this simulation is confirmed.

### 4. The cycle simulation

In the case of the cycle simulation, by incorporating the evaporator simulation with lubricant oil, each predicted accuracy is shown to improve from  $\pm 20\%$  to  $\pm 10\%$  in the

cooling capacity, from  $\pm 20\%$  to  $\pm 8\%$  in COP, and from  $\pm 50\%$  to  $\pm 15\%$  in pressure loss.

## NOMENCLATURE

L ; length, m  
 $\phi$  ; void fraction  
 $\phi'$  ; inhibition coefficient of heat transfer  
G ; mass flux, kg/m<sup>2</sup>s  
S ; slip ratio  
S' ; nucleate boiling suppression factor  
 $\beta$  ; volume ratio  
Re; Reynolds number  
We ; Weber number  
 $\phi$  ; multiplier factor  
D ; inner diameter, m  
 $\alpha$  ; heat transfer coefficient, J/m<sup>2</sup>K  
F ; two phase flow doubling coefficient  
Pr; Prandtl number  
Bd ; bond number  
x ; vapor quality  
OCR ; lubricant oil mass percent %  
j ; j factor  
 $\rho$  ; density kg/m<sup>3</sup>  
Cp; constant pressure specific heat, kJ/kgK  
 $\sigma$  ; surface tension, N/m  
g; gravity  
 $\lambda$  ; thermal conductivity  
q; heat flux  
X<sub>tt</sub>; Lockhart and Martinelli Parameter

## Subscripts

ac ; acceleration  
g ; gas  
l ; liquid  
in ; inlet  
out ; outlet  
con ; convective  
bo ; boiling  
sat ; saturation  
v ; vapor  
TP ; two phase

## REFERENCES

- (1) S.Koyama, K.Kuwabara, 2004, Proc. JSRAE Annual Conf, A204-1-A204-2 (in Japanese)
- (2) T.Yamada, E.Hihara, 2004, Proc. JSRAE Annual Conf, B111-1-4 (in Japanese)
- (3) Katsuta.M, 2006, Proc. JSRAE Annual Conf, B116(in Japanese)
- (4) Chen,J.C. 1966, Chem. Pro. Design Dev. vol.5(3), 322-329
- (5) Y.Chang, C.Wang,1997, International Journal of Heat and Mass Transfer Vol. 40, No.3 533-544
- (6) S.Koyama, K.Kuwabara,2006, 43<sup>rd</sup> National Heat Transfer Symposium of Japan, A122